Computers and Chemical Engineering 34 (2010) 900–913

Contents lists available at ScienceDirect

Computers and Chemical Engineering

journal homepage: www.elsevier.com/locate/compchemeng

MPEC strategies for cost optimization of pipeline operations

B.T. Baumrucker, L.T. Biegler*

Chemical Engineering Department, Carnegie Mellon University, Pittsburgh, PA 15213, USA

ARTICLE INFO

Article history:
Received 10 April 2009
Received in revised form 23 July 2009
Accepted 26 July 2009
Available online 3 August 2009

Keywords:
Pipeline optimization
Electricity pricing
Dynamic optimization
Complementarity
MPEC
Nonlinear programming

ABSTRACT

This study develops a mathematical program with equilibrium constraints (MPECs) approach for efficient operation of gas pipelines. The resulting model handles time dependent operations in order to determine minimum energy consumption and operating cost over a given time horizon. The MPEC structure also allows flow reversals, flow transitions and other nonsmooth elements to be incorporated within the approach. Applied to industrial gas pipelines, this approach can also deal with customer demand satisfaction in the presence of compressor outages and minimize recovery time for systems that are unable to meet customer demands at all times. A large-scale oxygen pipeline case study is considered to demonstrate this approach and complex energy pricing schemes are also applied to this problem. These schemes include time of day electricity pricing, along with extensions to Real Time Pricing and Day Ahead Pricing. Compared to flat rate and minimum energy optimizations, respectively, we observe operating cost savings up to 5.13% for time of day electricity pricing and up to 12.85% for Real Time Pricing.
© 2009 Elsevier Ltd. All rights reserved.

1. Introduction

Industrial gases such as oxygen and nitrogen are consumed in large quantities by the steel and chemical industries, while hydrogen is used in large quantities in chemical and petroleum refining industries. When these industrial gas customers are located in close proximity, pipelines are the delivery method of choice. However, the efficient operation of such pipeline networks is not as straightforward as other chemical processes and has been the subject of much study over the last several decades.

Heuristics for the operation of natural gas transmission pipelines were proposed as early as 1961 (Batey, Courts, & Hannah, 1961). However natural gas transmission pipelines differ from industrial gas networks in key ways. Transmission lines are long lines with minimal branching. Industrial gas networks are distribution systems with significant branching. Furthermore transmission lines carry gas across geographic regions and almost always have their flow direction predetermined, whereas distribution systems can have multiple sources and sinks in the network and the direction of flow may change in time. In Marqués and Morari (1988), an on-line optimization of transmission lines is considered by linking a dynamic simulator with a quadratic programming package. More recently Larnaes (2004) discusses how optimization can be used to improve carrying capacity of constrained pipelines and as a decision support tool during unusual situations, such as planned or unplanned outages. Zhu, Henson, and Megan (2001), consider a linear model predictive control (LMPC) framework for oxygen pipeline networks. Their model was based on nodal equations to represent flows between pipe segments, thus leading to a nonlinear ODE model that was later simplified for the LMPC controller. However, flow reversals could not be considered due to network topology and simpler friction factor models. Ierapetritou, Wu, Vin, Sweeney, and Chigirinskiy (2002) consider scheduling air separation plant modes of operation with highly variable and uncertain energy costs, but do not consider the effects of scheduling on transportation cost. van den Heever and Grossmann (2003) consider integrated planning and scheduling (but not control) of hydrogen production and transportation through pipeline networks, while explicitly allowing flow reversals in their network formulation and complex energy pricing schemes. More generally Shobrys and White (2000) discuss the more challenging issue of integrated planning, scheduling and control in industry.

The next section presents a brief review of MPEC strategies solved with NLP methods. Section 3 develops the problem statement for the pipeline optimization model, while Section 4 describes a number of relevant electricity pricing schemes. A case study that combines these two topics and demonstrates the MPEC solution is presented in Section 5 while concluding remarks are made in Section 6.

2. Complementarities for nonsmooth behavior

Optimization of systems with nonsmooth conditions requires special treatment within the problem formulation. Here, Mixed

* Corresponding author. Tel.: +1 412 268 2232; fax: +1 412 268 7139.
E-mail address: lb01@andrew.cmu.edu (L.T. Biegler).

0098-1354/$ – see front matter © 2009 Elsevier Ltd. All rights reserved.
doi:10.1016/j.compchemeng.2009.07.012

Integer Programming (MIP) and Generalized Disjunctive Programming (GDP) strategies are general ways to handle logical disjunctions that lead to nonsmoothness. However, the associated computational expense may be high for large and dynamic systems with many discrete decisions. This is often the case in dynamic systems with switches that may occur at any point in time. Because worst-case MIP solution time grows exponentially with the number of discrete decisions, complementarity formulations offer an alternative for some classes of disjunctive problems. Complementarity is a relationship between two variables where either one (or both) must be at its bound. Complementarities are particularly useful in optimization since they can be used to model disjunctions without the use of binary variables. As a result, they can be embedded within a standard nonlinear programming (NLP) solver to obtain fast local solutions, generally in polynomial time. On the other hand, the introduction of complements introduces an inherent nonconvexity as well as linear dependence of active constraints at all feasible points.

For nonsmooth systems, complementarity models allow a number of options when dealing with disappearance of phases, flow reversal, safety valve operation, and other discrete events. For a more complete discussion of chemical engineering applications that can be modeled with complementarities, see Baumrucker, Renfro, and Biegler (2008) and Raghunathan and Biegler (2003). Algorithms for nonsmooth optimization tend to be less advanced and slower to converge than algorithms for NLPs.

A mathematical program with equilibrium constraints (MPECs) is often written as the following optimization problem with complementarity constraints:

$$min \quad f(z) \tag{1a}$$

$$s.t. \quad h(z) = 0 \tag{1b}$$

$$g(z) \geq 0 \tag{1c}$$

$$0 \leq z_1 \perp z_2 \geq 0 \tag{1d}$$

where we define complementing variables $z_1, z_2 \in \mathbb{R}^{n_1}$, as a subset of the variable vector, $z \in \mathbb{R}^{n_z}$ and $\perp$ is the complementarity operator enforcing at least one of the complementing bounds to be active. The complementarity constraint therefore implies the following:

$$z_1^{(j)} = 0 \quad \text{OR} \quad z_2^{(j)} = 0, \qquad j = 1, \ldots, n_1,\ z_1 \geq 0,\ z_2 \geq 0$$

so that complementarity constraints implicitly model disjunctive behavior. Here the OR operator is inclusive as both variables may be zero. This MPEC problem can then be reformulated using a variety of techniques and solved with a standard NLP solver (Anitescu, Tseng, & Wright, 2007; Baumrucker et al., 2008; Fletcher & Leyffer, 2004; Hu & Ralph, 2004; Leyffer, Lopez-Calva, & Nocedal, 2006; Raghunathan & Biegler, 2003, 2005; Ralph & Wright, 2004). For this study we rely mainly on a strategy based on a penalty formulation. This allows us to rewrite (1) through an ℓ_1 penalty function, leading to an NLP given by:

$$\text{PF}(\rho): \quad min \quad f(z) + \rho z_1^T z_2 \tag{2a}$$

$$s.t. \quad h(z) = 0 \tag{2b}$$

$$g(z) \geq 0 \tag{2c}$$

$$z_1, z_2 \geq 0 \tag{2d}$$

Here the complementarity is moved from the constraints to the objective function and the resulting problem is solved for a suitably large value of ρ. If $\rho \geq \rho_c$, where ρ_c is the critical value of the penalty parameter, then the complementarity constraints will be satisfied at the solution. Similarly, Anitescu et al. (2007) consider a related "elastic mode" formulation, where artificial variables are introduced to relax the constraints in PF(ρ) and an additional ℓ_∞ constraint penalty term is added. In both cases the resulting NLP formulation has the following properties:

- If z^* is a strongly stationary point for (1), then for all ρ sufficiently large z^* is a stationary point for PF(ρ) (Ralph & Wright, 2004).
- If z^* is a solution to PF(ρ) and z^* is feasible for (1) with finite ρ, then z^* is a strongly stationary solution to (1) (Anitescu et al., 2007).

These properties indicate that the exact penalty-based solution strategy is attracted to strongly stationary points for sufficiently large values of ρ, although these values may need to be determined by trial and error. Nevertheless, with a finite value of $\rho > \rho_c$ this ℓ_1 penalization is exact in the sense that all strongly stationary points of (1) are local minimizers to PF(ρ). Therefore, PF(ρ) allows any general nonlinear programming solver to be used to solve a complementarity problem. This approach is described in more detail in Anitescu et al. (2007) and Leyffer et al. (2006). In addition to PF(ρ), we consider a simple smoothing strategy for specific terms in system equations that are once but not twice differentiable. Unlike standard smoothing approaches for MPECs (Ralph & Wright, 2004), an asymptotic solution of the smoothing parameter is not needed, as the first order optimality conditions are unaffected by the smoothing. Additional examples of MPECs applied to engineering optimization problems can be found in Baumrucker et al. (2008), Raghunathan, Diaz and Biegler (2004), Kameswaran, Staus and Biegler (2005) and Raghunathan, Perez-Correa, Agosin and Biegler (2006). To solve the resulting MPEC formulation, we apply the active set NLP solver, CONOPT (Drud, 2004). CONOPT quickly detects active sets and handles dependent constraints efficiently.

3. Problem statement and model

Industrial gas pipeline systems consist of suppliers and customers connected through a pipeline network subject to supplier capacity, customer demand, and constraints representing the physics of the pipeline. The dynamic behavior of the system affects the operation, pricing, and inventory. In particular the pipeline inventory, often referred to as *linepack*, allows the pipeline to respond to short term disruptions or upsets to the system. The goal of this study is to meet customer demands when possible at minimum operating cost, particularly when subject to complex energy pricing schemes. As a result, faster dynamics (such as flow controllers) are neglected.

Arcs $i \in I$ in the network represent pipe segments. Nodes $j \in J$ are located at the intersections of pipe segments. Properties for the pipe segment are assumed to be uniform throughout the segment. The model is defined over the set of discrete points in time, $t \in T$. Sets S and D are supplies (flows into the network) and demands (flows out of the network). Nomenclature for sets, parameters, and variables can be found in Table 1.

3.1. Pipe segment equations

In order to model and influence pipe segment inventories and deal with flow reversals within these segments, we begin with a partial differential equation (PDE) model of the pipe network. Consider the material balance equation (PDE form) assuming ideal gas behavior and isothermal conditions:

$$\frac{MWA}{RT}\frac{\partial P}{\partial t} + \frac{\partial q}{\partial z} = 0$$

For any given pipe segment, the material balance equation is a linear first order partial differential equation. For the purposes of operating cost optimization, it was determined that the solution of a PDE model would be prohibitively expensive to solve. Instead, a

Table 1
Nomenclature

Set definitions	
I	arcs (pipe segments) in the pipeline network
J	nodes (intersection of pipe segments) in the pipeline network
$K = \{in, out\}$	endpoints of pipe segment designated inlet/outlet
$T = \{0, 1, \ldots, t_f\}$	time points
$T_{on} \subset T$	on-peak time points
$T_{off} \subset T$	off-peak time points
D	demands in network
S	suppliers in network
$ArcToNode(I, J)$	set mapping of pipeline arcs I into node J
$ArcFromNode(I, J)$	set mapping of pipeline arcs I out of node J
$Supply(S, J)$	set mapping of supply nodes S to nodes in the network J
$Demand(D, J)$	set mapping of demand nodes D to nodes in the network J
Parameters	
A_i	cross-sectional area in arc i
C_p	constant pressure heat capacity of gas
D_i	diameter of pipe segment in arc i
L_i	length of pipe segment in arc i
MW	molecular weight
R	gas constant
T_{ref}	reference temperature for pipeline and compressor calculations
t_t	time elapsed from initial time at time point t in set T
ϵ_i	surface roughness of pipe in arc i
γ	ratio of constant pressure and constant volume heat capacities
η	thermodynamic efficiency of compressors
μ	viscosity of gas
Variables	
$\frac{dP}{dz}_{i,k,t}$	partial derivative of pressure with respect to position in arc i at endpoint k at time t
$f_{i,k,t}$	friction factor for gas in arc i at endpoint k at time t
$f^{lam}_{i,k,t}$	laminar friction factor for gas in arc i at endpoint k at time t
$f^{turb}_{i,k,t}$	turbulent friction factor for gas in arc i at endpoint k at time t
$mass_{i,t}$	mass in arc i at time t
$P^{node}_{j,t}$	pressure at node j at time t
$P_{i,k,t}$	pressure for arc i at endpoint k at time t
$P^{supply}_{j,t}$	supply pressure at node s at time t
$P^{demand}_{j,t}$	demand pressure at node d at time t
$\bar{P}_{i,t}$	average pressure in arc i at time t
$Power_{s,t}$	power used to compress gas for supply at node s at time t
$q_{i,k,t}$	mass flow rate for arc i at inlet/outlet k at time t
$q^{slack}_{d,t}$	slack flow rate at node d at time t
$q^{customer}_{d,t}$	customer flow rate at node d at time t
$q^{switch}_{d,t}$	flow rate switching variable at node d at time t
$q^{supply}_{s,t}$	supply flow rate at node s at time t
$q^{demand}_{d,t}$	demand flow rate at node d at time t
$Re_{i,k,t}$	Reynolds number for gas in arc i at endpoint k at time t

multi-period solution technique was proposed and implemented. The multi-period approach solves the problem using an integrated form of the material balance equation. The material balance equation in multi-period form is as follows:

$$\frac{MWA_iL_i}{RT_{ref}}(\bar{P}_{i,t+1} - \bar{P}_{i,t}) = \int_t^{t+1} (q_i^{in} - q_i^{out})dt \quad \forall i \in I, t \in T$$

where $\bar{P}_{i,t}$ represents the average pressure in the pipe segment i at time t. Since model equations are only written for the time points t and at the endpoints of the pipe segment, the integral on the right hand side of the equation can only be evaluated using explicit Euler, implicit Euler, or the trapezoidal rule. In particular, trapezoidal rule provides the highest accuracy of the three mentioned methods and is roughly equivalent to assuming the flow rates are piecewise continuous linear functions in time. Here the trapezoidal rule is used and the resulting material balance equations takes the following form:

$$\frac{MWA_iL_i}{RT_{ref}}(\bar{P}_{i,t+1} - \bar{P}_{i,t}) = \frac{1}{2}[(q_{i,in,t} - q_{i,out,t}) + (q_{i,in,t+1} - q_{i,out,t+1})](t_{t+1} - t_t) \quad \forall i \in I, t \in T \setminus \{t_f\} \tag{3}$$

The momentum balance equation for one-dimensional plug flow takes the following form:

$$\frac{dP}{dz} = \frac{-fRTq|q|}{2DA^2MWP}$$

The flow rates are available at the inlet and outlet of a pipe segment and the equation will need to be evaluated at both ends. For notational convenience the set $K = \{in, out\}$ is introduced and used to more compactly write equations that will need to be evaluated at both ends of the pipe segment. The momentum balance equation becomes:

$$\frac{dP}{dz}_{i,k,t} = \frac{-f_{i,k,t}RT_{ref}q_{i,k,t}|q_{i,k,t}|}{2D_iA_i^2MWP_{i,k,t}} \quad \forall i \in I, t \in T, k \in K \tag{4}$$

From the momentum balance equation we assume that the pipe segment is sufficiently long that friction contributions (using the Darcy–Weisbach friction factor) dominate the other contributing factors. This is a nonlinear first order differential equation. Furthermore, to model flow reversals we include a nonsmooth absolute value operator which requires a complementarity reformulation. An energy balance equation is not included, as we assume that pipe segments are sufficiently long to allow gas temperature to equilibrate to the ambient temperature. We therefore make an isothermal assumption; temperature is set to $T_{ref} = 298.15$ K.

3.2. Node equations

A material balance equation is written for each node:

$$\sum_{i:(i,j)\in ArcToNode(I,J)} q_{i,out,t} + \sum_{s:(s,j)\in Supply(S,J)} q^{supply}_{s,t} = \sum_{i:(i,j)\in ArcFromNode(I,J)} q_{i,in,t} + \sum_{d:(d,j)\in Demand(D,J)} q^{demand}_{d,t} \quad \forall j \in J \tag{5}$$

The network node represents a junction in the actual physical pipe network. This physical junction has no appreciable volume. Hence the node material balance has no accumulation term and sets the flows into the node equal to the flow out of it.

Pressure balances require the pressures to be continuous at each node:

$$P_{i,out,t} = P^{node}_{j,t} \quad \forall (i,j) \in ArcToNode(I,J), t \in T \tag{6}$$

$$P_{i,in,t} = P^{node}_{j,t} \quad \forall (i,j) \in ArcFromNode(I,J), t \in T \tag{7}$$

$$P^{supply}_{s,t} = P^{node}_{j,t} \quad \forall (s,j) \in Supply(S,J), t \in T \tag{8}$$

$$P^{demand}_{d,t} = P^{node}_{j,t} \quad \forall (d,j) \in Demand(D,J), t \in T \tag{9}$$

The pressure continuity equations set the node pressure equal to the pressure either into or out of the connected pipe line arc. The equations further enforce that all flows into or out of a node have the same pressure. The supply and demand pressures are also determined by the appropriate node pressures.

3.3. Other network equations

The compressor power is calculated by:

$$Power_{s,t} = q_{s,t}^{supply} \frac{C_p T_{ref}}{\eta} \left[\left(\frac{P_{s,t}}{P_{inlet}} \right)^{(\gamma-1)/\gamma} - 1 \right] \quad \forall s \in S, t \in T \tag{10}$$

where P_{inlet} is the inlet suction pressure. The compressor power equation is valid for adiabatic compression of a polytropic gas.

3.3.1. Constitutive equations

Reynolds number

$$Re_{i,k,t} = \frac{|q_{i,k,t}| D_i}{\mu A_i} \quad \forall i \in I, k \in K, t \in T \tag{11}$$

Laminar friction factor

$$f_{i,k,t}^{lam} = \frac{64}{Re_{i,k,t}} \quad \forall i \in I, k \in K, t \in T \tag{12}$$

Colebrook–White equation for turbulent friction factor

$$f_{i,k,t}^{turb} = 1.326 \left[\ln \left(\frac{1}{\epsilon_i/(3.7D_i) + 2.51/\left(Re_{i,k,t} \sqrt{f_{i,k,t}^{turb}} \right)} \right) \right]^{-2} \quad \forall i \in I, k \in K, t \in T \tag{13}$$

Average pressure calculation

$$\bar{P}_{i,t} = \frac{\int_0^{L_i} P(z')dz'}{\int_0^{L_i} dz} = \frac{\int_0^{L_i} \left(P_0 + \int_0^{z'} \left(\frac{dP}{dz} \right) dz \right) dz'}{L_i} \quad \forall i \in I, t \in T$$

3.4. Collocation equations

The momentum balance (4) is a first order nonlinear differential equation in space. This equation has to be discretized spatially in a suitable fashion, in order to be used in an optimization model. Orthogonal collocation on finite elements is the method chosen for this study. However the multi-period nature of the model poses a unique challenge to implementing such a scheme. The differential equation is a function of flow rate and it is expected that the flow rate would change continuously throughout the pipe segment as its pressure changes. However, no descriptive equation describes the flow rate as a function of position in the pipe. (Outside of the multi-period context, the PDE mass balance equation would describe this behavior.)

The selection of collocation schemes is therefore limited to methods that only require derivative information at either endpoint or both endpoints, i.e., 1-point Radau or 2-point Lobatto. For this study, Hermite cubic polynomials are used as the basis functions for the 2-point Lobatto collocation as described in Finlayson (2003). Another choice of basis functions would have been possible, but the Hermite polynomials were chosen for their ease of use. The basis functions are:

$$H_1 = (1-\xi)^2(1+2\xi)$$
$$H_2 = \xi(1-\xi)^2 L$$
$$H_3 = \xi^2(3-2\xi)$$
$$H_4 = \xi^2(\xi-1)L$$

The functions are defined here on the normalized interval of $\xi = (z/L) \in [0, 1]$. Note that at $\xi = 0$ all functions vanish except H_1. Furthermore, the derivatives of the functions all vanish at $\xi = 0$ except H_2. Similar relations hold at $\xi = 1$ for H_3 and H_4. The differential equation and integrated function are represented by linear combinations of these values:

$$P(\xi) = \sum_{i=1}^{4} a^i H^i(\xi)$$
$$\frac{dP}{dz} = \frac{1}{L} \sum_{i=1}^{4} a^i \frac{dH^i}{d\xi}$$

This leads to the following relationship between the coefficient values a^i and model variables defined $\forall i \in I, t \in T$:

$$P_{i,in,t} = a_{i,t}^1 \tag{14}$$

$$\frac{dP}{dz}_{i,in,t} = a_{i,t}^2 \tag{15}$$

$$P_{i,out,t} = a_{i,t}^3 \tag{16}$$

$$\frac{dP}{dz}_{i,out,t} = a_{i,t}^4 \tag{17}$$

For 2-point Lobatto collocation, the pressure approximation takes the form:

$$a_{i,t}^3 = a_{i,t}^1 + \frac{L_i}{2}(a_{i,t}^2 + a_{i,t}^4) \quad \forall i \in I, t \in T \tag{18}$$

These coefficients can then be used to calculate $\bar{P}$ in (3) directly:

$$\bar{P}_{i,t} = \frac{\int_0^{L_i} P(z)dz}{\int_0^{L_i} dz} = \frac{(1/2)a_{i,t}^1 + (1/12)a_{i,t}^2 L_i + (1/2)a_{i,t}^3 - (1/12)a_{i,t}^4 L_i}{L_i} \quad \forall i \in I, t \in T \tag{19}$$

3.5. Complementarities

The absolute value operator is present in the momentum balance and the Reynolds number calculation. The resulting functions are nonsmooth and will violate the assumptions made by traditional NLP solvers. Instead, a smooth complementarity formulation is used. The absolute value operator can be modeled as:

$$|q_{i,k,t}| = q_{i,k,t}^+ + q_{i,k,t}^- \quad \forall i \in I, k \in K, t \in T \tag{20}$$

$$q_{i,k,t} = q_{i,k,t}^+ - q_{i,k,t}^- \quad \forall i \in I, k \in K, t \in T \tag{21}$$

$$0 \le q_{i,k,t}^+ \perp q_{i,k,t}^- \ge 0 \quad \forall i \in I, k \in K, t \in T \tag{22}$$

where the last line represents a complementarity relationship, and either of the two inequalities (or both) must hold as equality.

As noted above, complementarity terms from (1) are reformulated using (2). However, for complementarities derived from the absolute value operator, we apply a smoothing formulation instead, i.e., $q_{i,k,t}^+ q_{i,k,t}^- = \epsilon$, as this term appears only in (4) and (11). This leads to a slight inaccuracy at very low Reynolds numbers, but serves to keep the friction factor bounded in (12). Moreover, for a sufficiently small value of ϵ the pressure–flow relationships remain unaffected; from (12) and (4) we see that the absolute value quantities cancel. So even though the calculation of $|q_{i,k,t}|$ is approximated, Eq. (4) will be calculated correctly.

Complementarities can also be used to represent piecewise functions. The friction factor is defined differently for different ranges of Reynolds number. In particular:

$$f = \begin{cases} f_{i,t}^{lam} & Re < 2300 \\ f_{i,t}^{turb} & Re > 2300 \end{cases}$$

This type of behavior can be modeled with complementarity constraints. The complementarity constraints for this particular problem are derived from the following equation:

$$f_{i,t} = u_{i,t} f_{i,t}^{lam} + (1 - u_{i,t}) f_{i,t}^{turb}$$

and the stationarity conditions of the following minimization problem:

$$\begin{aligned} &min_{u_{i,t}} \quad u_{i,t}(Re_{i,t} - 2300) \\ &s.t. \quad 0 \le u_{i,t} \le 1 \end{aligned}$$

By inspection it can be seen that if the Reynolds number is greater than 2300, the minimization problem will set the switching variable $u_{i,t}$ to zero and the friction factor equal to the turbulent value. A similar analysis holds for Reynolds numbers less than 2300. The stationarity conditions of this minimization problem $\forall i \in I$, $k \in K$, $t \in T$ are given by:

$$\begin{aligned} &f_{i,k,t} = u_{i,k,t} f_{i,k,t}^{lam} + (1 - u_{i,k,t}) f_{i,k,t}^{turb} \\ &(Re_{i,k,t} - 2300) - \lambda_{i,k,t}^{0} + \lambda_{i,k,t}^{1} = 0 \\ &0 \le u_{i,k,t} \perp \lambda_{i,k,t}^{0} \ge 0 \\ &0 \le (1 - u_{i,k,t}) \perp \lambda_{i,k,t}^{1} \ge 0 \end{aligned}$$

It should be noted that if the Reynolds number is exactly 2300, then the friction factor calculation becomes set valued. In particular, the value of $f_{i,t}$ can take any convex combination of the laminar and turbulent values.

Alternatively, the friction factor could be defined with more than two piecewise segments. One common scheme involves using laminar values for Reynolds numbers below 2100, turbulent values for numbers greater than 4000, and a linear interpolation for values in between the two. This type of behavior can also be modeled using complementarities. One key advantage of this approach is that at the two switching points in the piecewise function definition the friction factor is continuous and the transition region interpolation matches the laminar and turbulent friction factors at the switching points. A convex combination at these switching points is then single valued and not set valued, as in the prior case. Generalizing the complementarity formulation to this interpolation leads to the following form $\forall i \in I$, $k \in K$, $t \in T$:

$$f_{i,k,t} = u_{i,k,t}^{1} f_{i,k,t}^{lam} + u_{i,k,t}^{2} f_{i,k,t}^{trans} + u_{i,k,t}^{3} f_{i,k,t}^{turb} \tag{23a}$$

$$(Re_{i,k,t} - 2100) + \gamma_{i,k,t} - \lambda_{i,k,t}^{1} = 0 \tag{23b}$$

$$(Re_{i,k,t} - 2100)(Re_{i,k,t} - 4000) + \gamma_{i,k,t} - \lambda_{i,k,t}^{2} = 0 \tag{23c}$$

$$(4000 - Re_{i,k,t}) + \gamma_{i,k,t} - \lambda_{i,k,t}^{3} = 0 \tag{23d}$$

$$u_{i,k,t}^{1} + u_{i,k,t}^{2} + u_{i,k,t}^{3} = 1 \tag{23e}$$

$$0 \le u_{i,k,t}^{1} \perp \lambda_{i,k,t}^{1} \ge 0 \tag{23f}$$

$$0 \le u_{i,k,t}^{2} \perp \lambda_{i,k,t}^{2} \ge 0 \tag{23g}$$

$$0 \le u_{i,k,t}^{3} \perp \lambda_{i,k,t}^{3} \ge 0 \tag{23h}$$

The complementarities for the piecewise definition of the friction factor are now reformulated using the PF(ρ) formulation described above.

4. Complex energy pricing

The price of energy depends on numerous factors including the form of energy provided, supply, demand, location and time of day. Energy providers often turn to complex pricing schemes to try to allocate resources to greatest effect. These complex pricing schemes lead to opportunities that are difficult, if not impossible, to exploit without the aid of modern optimization techniques.

In this study, we consider NLP formulations and solution strategies for optimizing operations of time dependent processes to reduce the cost of energy. A case study of an industrial gas pipeline is used to test and demonstrate the effectiveness of these strategies as well as illustrate some novel operating strategies for pipeline networks.

- The most common electricity pricing scheme is the *fixed rate structure*. This is the rate structure typically used for households. In this scheme the customer pays a fixed cost per kWh of energy used. Sometimes this is modified such that the cost is fixed per unit, but dependent on the customer's total usage or maximum demand. This tiered energy pricing scheme can be viewed as being represented by a function that is piecewise constant. Additionally with this scheme, there may be a charge based on maximum demand.
- *Time of day electricity pricing* divides the day into different rate periods, each with its own electricity price. The most common scheme involves two 12-h time periods. One is the peak electrical usage time period and the other is the off-peak time period. The electricity in the peak period costs more than electricity during the off-peak period. This pricing scheme may also have an additional charge based on maximum on- and off-peak demands or a tiered structure for on- and off-peak periods.
- *Day Ahead electricity pricing* is based on the pricing of electricity varying hourly. Approximately 24 h in advance, the utility company will publish hourly electricity prices for the next day. The price they charge is based on an estimate of what their costs will be to purchase the energy for each time period; this is essentially equivalent to a commodities futures contract price.
- *Real Time Pricing* also has hourly varying electricity prices, but the cost of electricity is based on the real time market balancing price, i.e., the last price paid by a utility company for electricity in that time period. This is equivalent to the spot price or clearing price.

The complex energy pricing aspect of this work could really be applied to any model, not just the pipeline model presented here, provided that it meets two criteria. The total billing energy usage must be quantifiable. In particular, this means that processes that share a utility bill cannot be optimized independently. Also, the model must be able to consider time dependence of the process and have variable inventory.

4.1. Motivation for complex energy pricing schemes

Electricity is not readily stored and must be used (or wasted) as it is produced. In order to maintain stable operation of the electrical grid, power plants must ramp up and down frequently in order to match generating capacity to current demand plus a safety margin.

Base load power plants (those that provide power during both peak and off-peak usage periods) such as coal and nuclear plants require hours or even days to change their power output. These plants typically have high capital costs, but relatively low operating costs making them well suited to run in constant operation. In contrast, peak load power plants, typically using natural gas, can change their power output in minutes. Additionally they typically have low capital requirements; however, they have relatively high operating costs. This makes them well suited to only operating when necessary. As a consequence, peak generating capacity may only be in operation for a few hundred hours per year. Clearly there is an economic incentive to shift electricity usage from peak time periods to off-peak time periods, thus resulting in the electricity being generated by the less expensive base load power plants. Complex electricity pricing schemes are a way to shift the economic incentive from the utility companies to consumers of power.

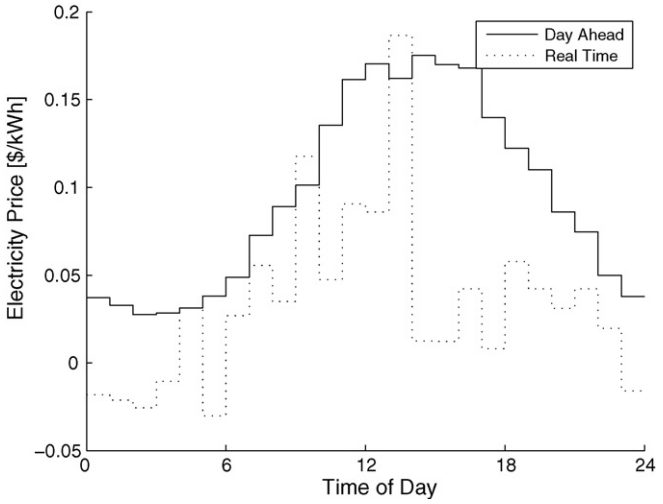

Fig. 1. Real Time Price and Day Ahead Price of electricity for East St. Louis on June 9th, 2008 Ameren-RTP.

Real time energy pricing can easily vary by an order of magnitude over the course of a day. This is especially true during hot summer days, when electricity demand is the highest. One interesting consequence of real time energy pricing as a spot market or clearing price is that the price of energy can go negative, and the customer can actually be paid to use electricity. This can occur because of the way the clearing price is set. Typically energy producers bid amounts of energy they wish to produce and the price they are willing to accept to produce it. An Independent System Operator acts as a clearinghouse and matches the purchases of energy with production. The lowest bids from producers are accepted until consumers' demand is satisfied. All producers receive the highest price bid that was accepted. If an energy producer is unable to ramp production down they may bid a negative price to ensure being selected with the expectation that a positive clearing price will still be set. However if too many producers do this, the clearing price may be set negative and producers will have to pay consumers to use their power. Obviously, this happens only when electricity demand is low compared to base load generating capacity, and this is likely seasonal.

Fig. 1 shows the Real Time Price and Day Ahead Price of electricity prices for East St. Louis on June 9th, 2008 Ameren-RTP. The Day Ahead Prices vary smoothly by a factor of six from off-peak to on-peak. The Real Time Prices oscillate sharply from $−0.03/kWh to $0.19/kWh and we observe that negative Real Time Prices actually occur. Further, the Day Ahead Price is in some sense a forecast of the Real Time Price, although the two behave differently.

4.2. Formulations to handle complex energy pricing schemes

Electricity rate plan data for this study come from Ameren, a utility company serving the greater St. Louis area. Rate plan and Real Time Price data can be found on their website Ameren-Rates, Ameren-RTP.

4.2.1. Tiered pricing

Tiered pricing can be represented as a piecewise linear function. Typically the total cost of electricity is the sum of the Customer Charge (CC), the Demand Charge (DC), and the Energy Charge (EC). The Customer Charge is typically a small fixed amount. The Demand Charge is a cost times the maximum Demand (D_{max}), in kW. The Energy Charge is piecewise linear; the domain for each piece is dependent either on the total energy used (E), in kWh, or some ratio of the energy used to maximum demand.

$$total\_cost = CC + DC + EC$$
$$CC = c_c$$
$$DC = c_d D_{max}$$
$$EC = \begin{cases} c_1 E & E \le 150D_{max} \\ c_2(E - 150D_{max}) + c_1(150D_{max}) & 150D_{max} \le E \le 350D_{max} \\ c_3(E - 350D_{max}) + c_2(200D_{max}) + c_1(150D_{max}) & 350D_{max} \le E \end{cases}$$

This piecewise linear function can be derived from the following minimization problem and associated equation:

$$\begin{array}{ll} min_{u^i} & (E - 150D_{max})u^1 + (E - 150D_{max})(E - 350D_{max})u^2 + (350D_{max} - E)u^3 \\ s.t. & u^1 + u^2 + u^3 = 1 \\ & u^i \ge 0 \quad i = 1, 2, 3 \end{array}$$

$$EC = u^1 f^1 + u^2 f^2 + u^3 f^3$$

From the stationarity conditions, we derive a complementarity formulation given by:

$$\begin{array}{l} EC = u^1 f^1 + u^2 f^2 + u^3 f^3 \\ (E - 150D_{max}) + \gamma - \lambda^1 = 0 \\ (E - 150D_{max})(E - 350D_{max}) + \gamma - \lambda^2 = 0 \\ (350D_{max} - E) + \gamma - \lambda^3 = 0 \\ u^1 + u^2 + u^3 = 1 \\ 0 \le u^1 \perp \lambda^1 \ge 0 \\ 0 \le u^2 \perp \lambda^2 \ge 0 \\ 0 \le u^3 \perp \lambda^3 \ge 0 \end{array}$$

where

$$\begin{array}{l} f^1 = c_1 E \\ f^2 = c_2(E - 150D_{max}) + c_1(150D_{max}) \\ f^3 = c_3(E - 350D_{max}) + c_2(200D_{max}) + c_1(150D_{max}) \end{array}$$

This complementarity formulation is embedded within the pipeline NLP with u^i as a switching variable, f^i as the function over each domain, γ as the KKT multiplier for the inner equality constraint and λ^i as the KKT multiplier for the inequality constraints. The complementarity operator $\perp$ indicates that either the switching variable or its multiplier must be at zero. Note that when $E < 150D_{max}$, the formulation sets $u^1 = 1$ and all other switching variables equation to zero, thus indicating this segment of the piecewise function is active. This likewise holds for the second and third pieces of the piecewise function. The associated equation then sets the variable EC equal to the appropriate piecewise function value.

4.2.2. Maximum demand

The maximum demand over time is modeled by an inequality constraint that ensures D_{max} is not less than the total power, along with a penalty term in the objective function that ensures an active inequality. To minimize the cost of energy the penalty term already exists in the objective function and an additional penalty term need not be added. The problem is formulated as follows:

$$min \quad (CC + EC) + c_d D_{max} \quad s.t. \quad D_{max} \ge \sum_{s \in S} Power_{s,t} \quad \forall t$$

This formulation is well suited to this problem as the penalty multiplier is actually the physically relevant demand charge. From the optimality condition, this positive demand charge is also the Lagrange multiplier for the associated inequality constraint, ensuring that it must be active for some t.

Time of day electricity pricing often requires the determination of both an on- and off-peak maximum demand value. The utility will then charge based on some function of these values. For instance, if the demand charge is calculated using the larger of the maximum on peak demand or half the maximum off-peak demand,

then the maximum demand value D_{max} can be calculated from:

$$\begin{aligned} min \quad & (CC + EC) + c_d D_{max} \\ s.t. \quad & D_{max} \geq \sum_{s \in S} Power_{s,t} \quad \forall t \in T_{on} \\ & D_{max} \geq \frac{1}{2} \sum_{s \in S} Power_{s,t} \quad \forall t \in T_{off} \end{aligned}$$

4.2.3. Rank ordering of peak demands

Instead of maximum peak usage, the billing demand may be based on the *i*th largest demands during the billing period (van den Heever and Grossmann, 2003). In this case, repeated use of the *min* and *max* functions can be used to determine the *i*th largest element of *n* elements.

$$min_j(\bar{d}_j), \quad \bar{d}_j = max(d_{j_1}, \ldots, d_{j_{n-i+1}}) = max(\Delta_j)$$

where d are the demands and the set Δ represents all possible combinations (Δ_j) of $n - i + 1$ elements from a set of n demands. For example the second highest element among four demands can be determined by:

$$min(max(d_1, d_2, d_3), max(d_2, d_3, d_4), max(d_1, d_3, d_4), max(d_1, d_2, d_4)).$$

This formulation for rank ordering of values is polynomial in the number of *min* and *max* operators required. When solved with a method that scales polynomially in time with problem size, it can be assumed that this formulation will still scale polynomially in solution time. However, for large i the polynomial scaling may be high order, since it requires $[(n) \ldots (n - i + 1)]/(i - 1)! - 1$ *min* or *max* operators to find the *i*th element among n elements.

The complementarities in all of these formulations would then need to be reformulated in order to use a standard NLP solver. This complementarity approach is expected to scale polynomially. Indeed, using the CONOPT solver we have observed a quadratic scale-up with problem size in Section 5.2.1.

5. Pipeline case studies

We now consider a series of case studies that demonstrate the utility of the proposed pipeline model. Here, network inventory refers to the *linepack* in the pipeline. Other types of inventory such as liquefied gas are not considered in this study.

The first set of case studies focus on demonstrating proof of concept for operational issues on a small pipeline network. In particular, we determine minimum compressor work for a scheduled compressor drop-out; this demonstrates the effect of the inventory on pipeline operations. Moreover, for compressor drop-out cases where it is not possible to meet customer demands, a modification of the model is proposed that determines the minimum recovery time. The second set of case studies focuses on the computational complexity and the effect of complex energy pricing on a pipeline of industrially relevant size. To determine the computational complexity, solution times are compared as the problem size increases. Subsequently optimal operating policies are determined and compared for flat rate, time of day, and real time electricity pricing plans. Upon discretization in time, all of these cases were formulated as MPECs and solved using the NLP formulation $PF(\rho)$ with $\rho = 1000$. Using the CONOPT solver, the resulting NLPs only needed to be solved once for this parameter value. This led to a very reliable MPEC solution strategy. All computation times are obtained on an Intel Q6600 machine with 8GB of RAM. No attempt was made to utilize more than one processor core for these calculations.

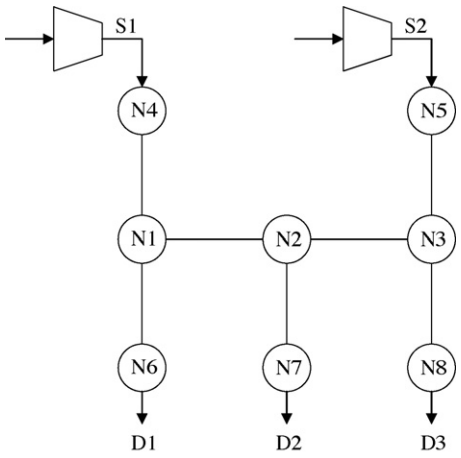

Fig. 2. Small network used in the case study. Nodes are labeled N#, sources are labeled S#, and demands (customers) are labeled D#.

5.1. Small network case studies

A network with two sources, three demands, seven arcs, and eight nodes was defined as shown in Fig. 2. All arcs were set to a length of 1000 m, diameter of 10 cm, and roughness (ϵ_i) of 50 μm in Eq. (13). Physical properties of natural gas were used and constant demands were set to 24 kg/h for each customer. The sources used an ambient temperature $T_{ref} = 298.15$ K and a compressor efficiency (η) of 85%.

5.1.1. Compressor drop-out

The system was examined over a set of 10 time periods each 1 h in length, with the network initially at steady state. The integral of the compressor power was minimized along with a penalty term, the sum of squares change in power from 1-h time period to the next with a regularization multiplier of 10. This regularization term smooths the compressor profiles. The resulting NLP can be written as:

$$\begin{aligned} min \quad & \sum_{s \in S} \int_{t=0}^{t=t_{end}} Power_{s,t} dt + 10 \sum_{s \in S} \sum_{t \in T \setminus \{0,6,7\}} (Power_{s,t} - Power_{s,t-1})^2 \\ s.t. \quad & \text{Eqs. (3)–(23)} \end{aligned}$$

The optimization was subject to minimum demand pressure of 500 kPa and a constraint that one of the compressors has a scheduled outage and performed no work at 6 h. Again, only inventory dynamics were considered and faster dynamics (such as flow controllers) are neglected. The NLP solver, CONOPT (Drud, 2004), returned compressor work values for each of the other time periods. The solver required 2.570 CPU seconds and 621 iterations to return the solution.

The minimum steady state work for this system is around 4.1 kW. The NLP solution shows a gradual increase in compressor work for both compressors, until 6 h. At this point, the compressor for S1 is taken off-line and the solution continues to increase the work on the compressor for S2. When the S1 compressor comes back on-line, its work is set to a level higher than the steady state value. The work on both compressors is then reduced in each subsequent time period; at 10 h, they are below their steady state values.

The optimal trajectory and network inventory is shown in Fig. 3. Initially the increased compressor work causes the overall network pressure and inventory to rise. The inventory rises until 6 h, when it begins to fall due to the off-line compressor. The depletion of inventory allows the network to meet the customer demand during the planned outage.

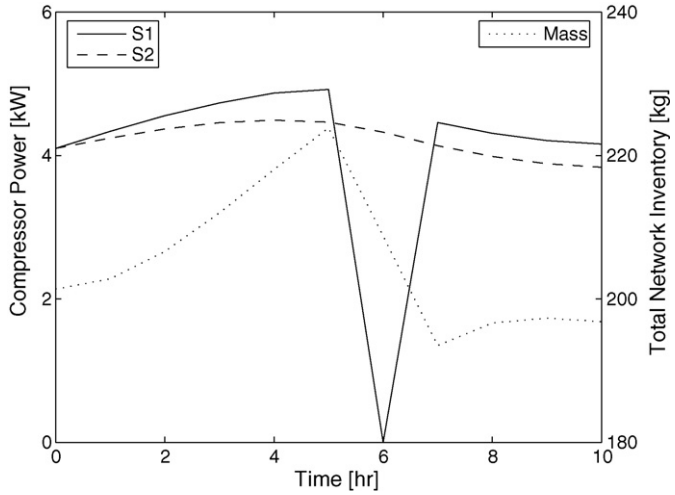

Fig. 3. Compressor power for S1 and S2 in kW and total network inventory in kg for small network compressor drop-out problem.

Several inequality constraints are active at the solution. In particular, the demand pressure is at its lower bound at nodes 6 and 7 at 7 h. as seen in Fig. 4. This is consistent with expectations since the pressure in the network would have dropped during the compressor outage in point 6. Furthermore, the demand pressure at node 7 is at its lower bound at 10 h. This indicates that the NLP solver has reduced the compressor to a level below the steady state minimum value and is slowly depleting inventory in the network. This is consistent with the observations made regarding the compressor work and inventory. Here the solver is taking advantage of the fact that no final time constraint has been posed for this problem.

5.1.2. Minimum recovery time

If the compressor outage is prolonged or if the compressor's flow rate is tightly constrained the preceding problem may not be feasible. Should this occur, customer flow rates would need to be cut in order to maintain minimum pressure specifications in the pipeline. However, control of demand flow rates are left to the customer. Furthermore, if the pressure should drop below the minimum, the regulatory system would automatically stop the flow to the affected customer, as depicted in Fig. 5.

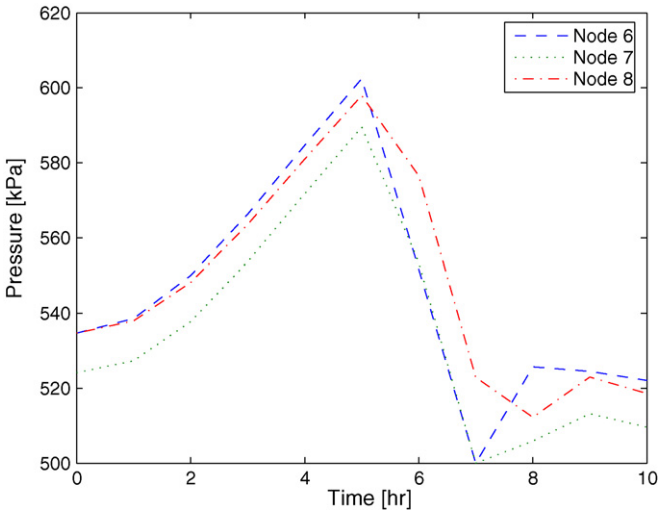

Fig. 4. Graph of pipeline pressure at demand nodes.

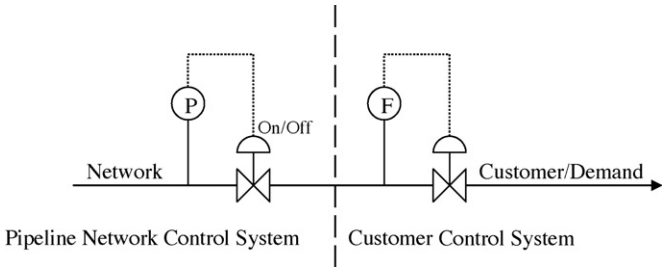

Fig. 5. Control system located at the network and customer boundary.

If the preceding problem is infeasible, it is desirable to add the regulatory control system of Fig. 5 and determine the minimum recovery time. This is the minimum amount of time where customer flows are less than customer demand. The control system can be described by using the following set of constraints defined by:

$$q_{d,t}^{demand} = q_{d,t}^{customer} + q_{d,t}^{slack} \quad d \in D, t \in T \tag{24}$$

$$\epsilon - q_{d,t}^{slack} - \lambda_{d,t}^{1} + \lambda_{d,t}^{2} = 0 \tag{25a}$$

$$0 \le \lambda_{d,t}^{1} \perp u_{d,t}^{switch} \ge 0 \tag{25b}$$

$$0 \le \lambda_{d,t}^{2} \perp (1 - u_{d,t}^{switch}) \ge 0 \tag{25c}$$

With ϵ set to a small positive constant (e.g., 10^{-8}) the variable u^{switch} takes a value of either zero or one, respectively, depending on whether customer demand is met or not. The NLP solver can then minimize the summation of $u_{d,t}^{switch}$ over its respective sets, and should also penalize the total slack flow rate. This is equivalent to minimizing response time for all customers.

The previous case was modified to demonstrate this minimum recovery time problem. The problem specifications are the same with the exception of the following. The compressor work was constrained to the range of 3.0–4.5. With these modifications, the NLP solver determined the minimum recovery time to be two customer time periods. In particular, nodes 6 and 7 were unable to meet customer demands during time period 6. The compressor profiles and flow rate slacks are given in Fig. 6. It was also determined that the customers will need to reduce their gas flow rates to 97% of their nominal values during this time period to prevent the pipeline pres-

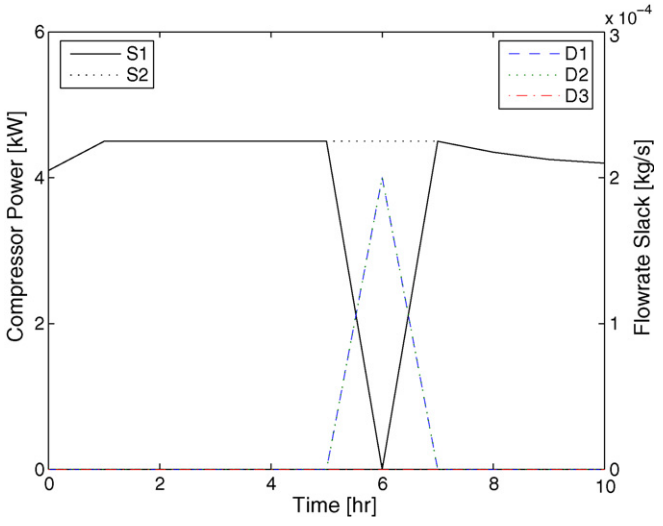

Fig. 6. Compressor power profiles and flow rate slacks for minimum recovery time case study.

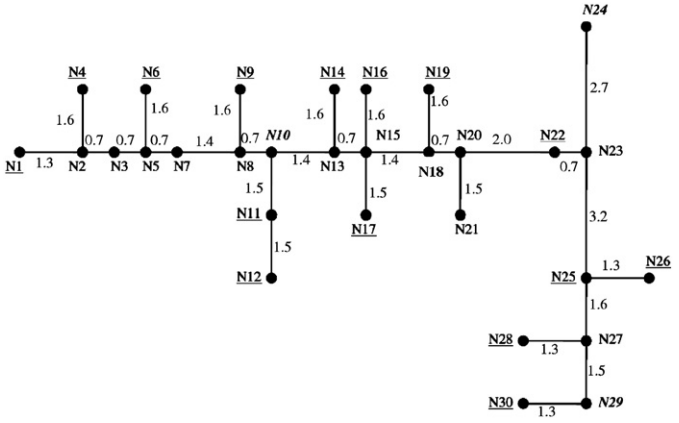

Fig. 7. Large network used in the case study. Pipe segment lengths are shown in *km*, nodes are labeled N#, with source nodes (suppliers) labeled in bold italics, and demand nodes (customers) underlined.

sure dropping to a point where the control system stops all flow to the customer.

CONOPT required 588 iterations and 2.460 s to determine that it is not possible to meet the customer demands subject to the specified constraints. The solver further required an additional 59 iterations and 0.300 s to determine the minimum recovery time.

5.2. Large network case studies

A large network with 3 sources, 15 demands, 29 arcs, and 30 nodes was defined as shown in Fig. 7. This fictitious network is based loosely on the actual pipeline network described in Zhu et al. (2001). All arcs were assumed to have a diameter of 10 cm, and roughness of $\epsilon_i = 50\,\mu$m. Physical properties of oxygen were used. The sources used an ambient temperature of 298.15 K and a compressor efficiency of 85%.

5.2.1. Scale-up of computations

An energy minimization problem was considered to examine the scaling of the problem. The objective function for this series of problems minimized the integral of the compressor power and a weighted regularization term, leading to the following optimization problem:

$$\min \sum_{s\in S}\int_{t=0}^{t=t_{end}} Power_{s,t}\,dt + 10^{-6}\sum_{s\in S}\sum_{t\in T\setminus\{0\}}(Power_{s,t}-Power_{s,t-1})^2$$
$$s.t. \quad \text{Eqs. (3)–(23)}$$

This problem is formulated as an NLP by approximating the time integral and differential equations with the trapezoidal rule. The problem was made arbitrarily large by increasing the number of 1-h time periods considered. The problems were initialized at steady state solutions for average customer demand. However, customer demand was assumed to be sinusoidal with a period of 2 π h and an amplitude of 5% of the nominal value. Furthermore, a final time constraint was added to the problem. In particular, the inventory in the network at final time must be at least as large as the inventory in the network at initial time.

$$mass_{i,t} = \frac{\bar{P}_{i,t} MWA_i L_i}{RT_{ref}} \quad \forall i \in I,\ t \in T \tag{26}$$

$$\sum_i mass_{i,0} \le \sum_i mass_{i,t_f} \tag{27}$$

Computational scaling results are presented in Table 2. The number of iterations required generally increases linearly with problem size. Furthermore, the computation time per iteration also increases linearly, leading to a quadratic increase in computation time as problem sizes increase.

5.2.2. Minimum cost with flat rate pricing

The large network problem is now modified to include an economic objective function using flat rate electricity pricing. The customer demands are assumed to be constant.

$$\min \quad \frac{CC+DC+EC}{1000} + Reg\times\delta + 10^6 \sum_{d\in D, t\in T} q_{d,t}^{slack} \tag{28a}$$

$$s.t. \quad CC = c_c \tag{28b}$$

$$DC = c_d D_{max} \tag{28c}$$

$$D_{max} \ge \sum_{s\in S} Power_t \quad \forall t \in T \tag{28d}$$

$$EC = \sum_{s\in S, t\in T\setminus\{t_f\}} \frac{1}{2}(Power_{s,t} + Power_{s,t+1})(t_{t+1}-t_t)cost_t \tag{28e}$$

Table 2
Large case study solution scaling results. Iterations increase approximately linearly while solution times increase quadratically. Variable, equation, and complementarity constraint counts are also presented.

Time periods	Iterations	Solution times [s]	Variables	Equations	Complementarity constraints
10	459	35.010	14,858	14,621	2552
15	642	65.520	21,598	21,266	3712
20	613	79.000	28,338	27,911	4872
25	1273	258.770	35,078	34,556	6032
30	1094	234.560	41,818	41,201	7192
35	1720	509.610	48,558	47,846	8352
40	1601	530.020	55,298	54,491	9512
45	2057	960.110	62,038	61,136	10,672
50	2343	919.170	68,778	67,781	11,832
55	1695	558.660	75,518	74,426	12,992
60	2153	994.200	82,258	81,071	14,152
65	1808	735.520	88,998	87,716	15,312
70	2655	1421.360	95,738	94,361	16,472
75	2462	1391.020	102,478	101,006	17,632
80	2775	1579.630	109,218	107,651	18,792
85	3271	2182.580	115,958	114,296	19,952
90	3661	3233.610	122,698	120,941	21,112
95	3485	3206.700	129,438	127,586	22,272
100	3507	2379.310	136,178	134,231	23,432

Table 3
Computation times and iteration results for the flat rate and time of day pricing case studies

Reg	Time [s]	Iterations
Flat rate		
1	1015.20	1082
10	885.57	868
100	1123.19	1534
Time of day		
1	1430.66	1411
10	1074.19	1023
100	980.07	899

$$\delta = \sum_{s \in S, t \in T \setminus \{t_f\}} \left(\frac{Power_{s,t+1} - Power_{s,t}}{t_{t+1} - t_t} \right)^2 \tag{28f}$$

$$\text{Eqs. (3)–(23), (24), (26) and (27)} \tag{28g}$$

For the particular flat rate pricing plan considered, $c_c = 217.25$, c_d =14.35 per kW, and $cost_t$ =0.024 per kWh $\forall t \in T$. The economic objective function requires that the optimization problem be formulated over a full billing period, typically 30 days, as the maximum demand value is defined over this billing period. In the prior section, the solution time of the pipeline problem was determined to increase approximately quadratically with the number of time periods. If the problem were increased to consider 720 hourly time periods for the billing period, the computations would become prohibitively expensive. Instead we choose a non-uniform time discretization, where small time periods are used initially and larger time periods are used further in the future. The problem then can be run more frequently, similar to a moving time horizon framework. In this implementation we used 12 1-h time periods followed by 6 2-h, 4 3-h, 3 4-h, and 56 12-h time periods. These were chosen such that future time periods are aggregated into blocks of on- and off-peak time periods. This discretization scheme resulted in a total of 81 time periods to consider a time horizon of 720 h (30 days).

The optimal trajectory was found for several different regularization parameters (*Reg*). Computation times and iterations results are shown in Table 3. A small regularization will only slightly smooth the compressor profiles and may lead to excessive wear on the process equipment or other operational problems not easily included in a mathematical programming context. In contrast a larger regularization will significantly smooth the compressor profiles, but may lead to excessively conservative and suboptimal operation. By judiciously choosing the regularization, the problem may be tuned to provide a reasonable trade-off between the various operational concerns. Figs. 8–11 show the effect of the regularization scheme on the optimal control profiles and network inventory. Note, the graphs focus on the first 3 days and the smaller time discretization, although the computation is considered the entire billing period. In all of these figures the pipeline initial condition is above its optimal steady state value. This is apparent by the initial decrease in both compressor work and network inventory followed by a leveling off of these values. Increasing the value of *Reg* has the effect of delaying and prolonging this transition. Specifically, for *Reg* = 1 the transition is complete after 12 h, while larger *Reg* values lead to transitions completed after 18 and 36 h. These optimal trajectories serve as base case scenarios, which will be compared to *time of day* optimal solutions in the next section.

5.2.3. Minimum cost with time of day pricing

The large network problem was then modified to include an economic objective function using time of day electricity pricing.

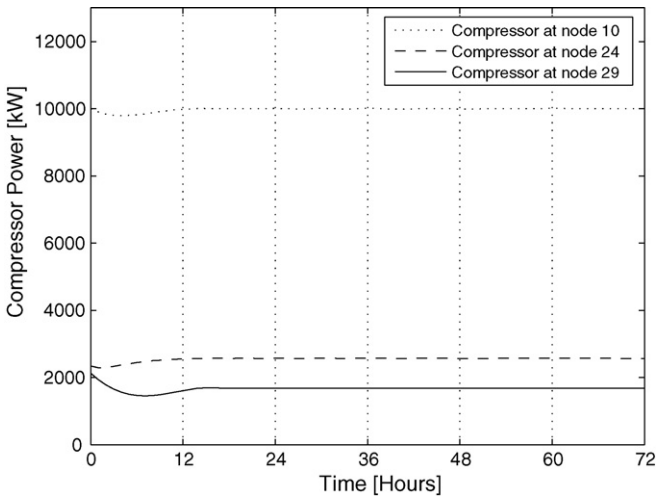

Fig. 8. Optimal compressor profiles for flat rate electricity pricing and a regularization parameter of 1.

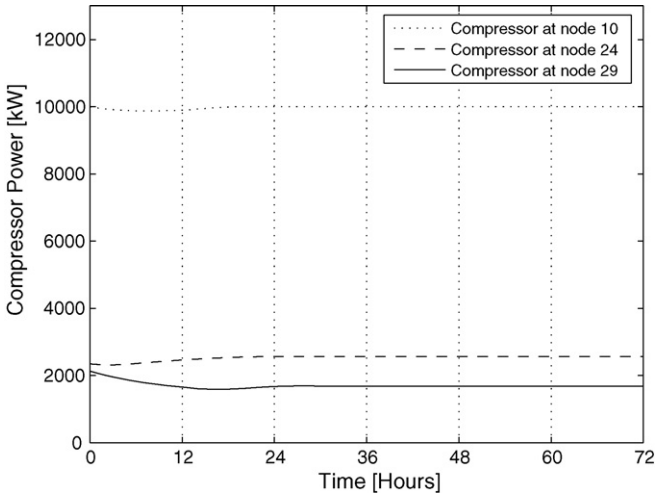

Fig. 9. Optimal compressor profiles for flat rate electricity pricing and a regularization parameter of 10.

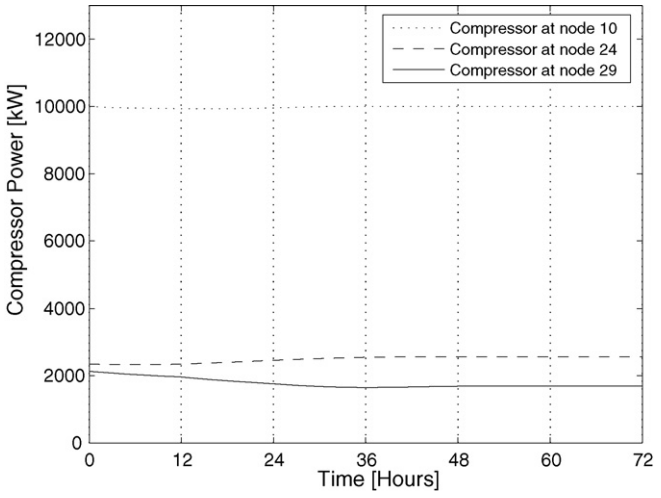

Fig. 10. Optimal compressor profiles for flat rate electricity pricing and a regularization parameter of 100.

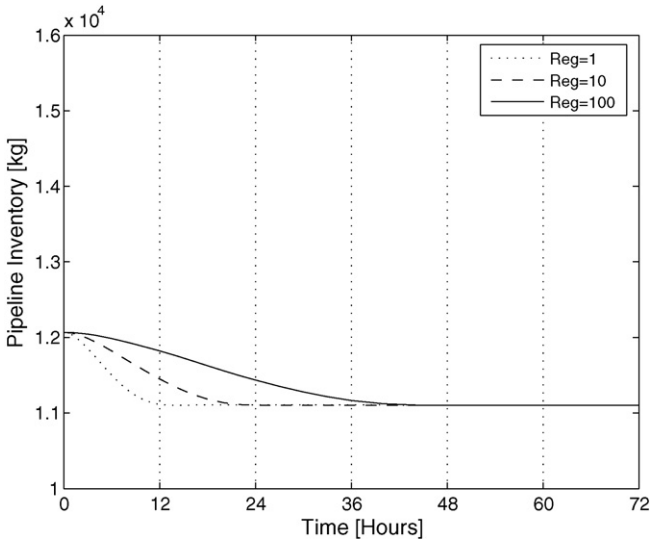

Fig. 11. Inventory profiles for flat rate electricity pricing for the three different regularization parameters considered.

The customer demands were assumed to be constant.

$$min \quad \frac{CC + DC + EC}{1000} + Reg \times \delta + 10^6 \sum_{d \in D, t \in T} q_{d,t}^{slack} \tag{29a}$$

$$s.t. \quad CC = c_c \tag{29b}$$

$$DC = c_d D_{max} \tag{29c}$$

$$D_{max} \geq \sum_{s \in S} Power_{s,t} \quad \forall t \in T_{on} \tag{29d}$$

$$D_{max} \geq \frac{1}{2} \sum_{s \in S} Power_{s,t} \quad \forall t \in T_{off} \tag{29e}$$

$$EC = \sum_{s \in S, t \in T \setminus \{t_f\}} \frac{1}{2}(Power_{s,t} + Power_{s,t+1})(t_{t+1} - t_t) cost_t \tag{29f}$$

$$\delta = \sum_{s \in S, t \in T \setminus \{t_f\}} \left(\frac{Power_{s,t+1} - Power_{s,t}}{t_{t+1} - t_t} \right)^2 \tag{29g}$$

$$\text{Eqs. (3)–(23), (24), (26) and (27)} \tag{29h}$$

For the particular time of day pricing plan considered, c_c = 231.42, c_d =14.35 per kW, $cost_t$ =0.0286 per kWh $\forall t \in T_{on}$, and $cost_t$ =0.0214 per kWh $\forall t \in T_{off}$. Note that the values of the cost coefficients c_c, c_d, and $cost_t$ are different in value from the prior case study. In particular, $cost_t$ in the prior example was equal for all t, but for the time of day pricing the coefficient takes either the on-peak or off-peak value depending on t. Furthermore, the value of D_{max} is calculated as the larger of the maximum on-peak demand or half the maximum off-peak demand. Just as in the flat rate electricity pricing, it is required that the optimization problem consider a full billing period, typically 30 days. The same non-uniform time discretization is used for this case study with the first 12-h time period at off-peak, the next 12 h at on-peak, and so on.

Computation times and iteration results are also shown in Table 3 for this case. As in the prior case study, the parameter *Reg* needs to be tuned to provide a reasonable trade-off between the various operational concerns. Figs. 12–15 show the effect of the regularization scheme on the optimal control profiles and network inventory. Note, the graphs focus on the first 3 days, although the computation considered the entire billing period. We also note that the demand charge has the effect of flattening the compressor power profiles during the on-peak time periods, but not during

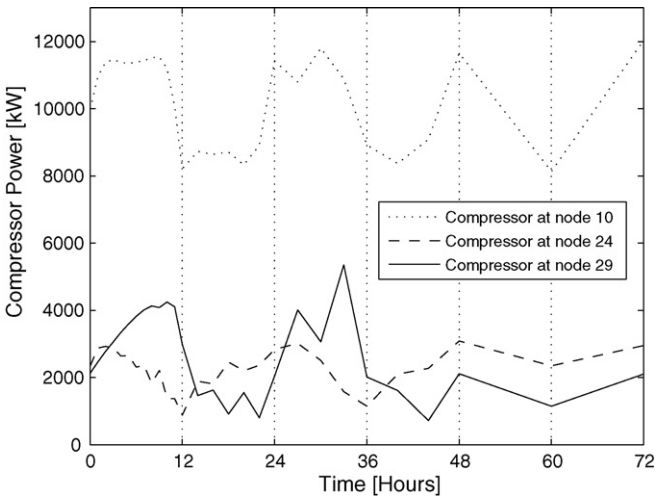

Fig. 12. Optimal compressor profiles for time of day electricity pricing and a regularization multiplier of 1.

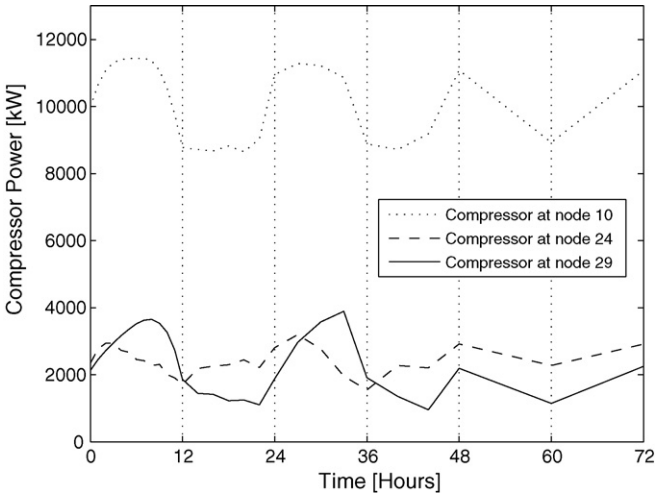

Fig. 13. Optimal compressor profiles for time of day electricity pricing and a regularization multiplier of 10.

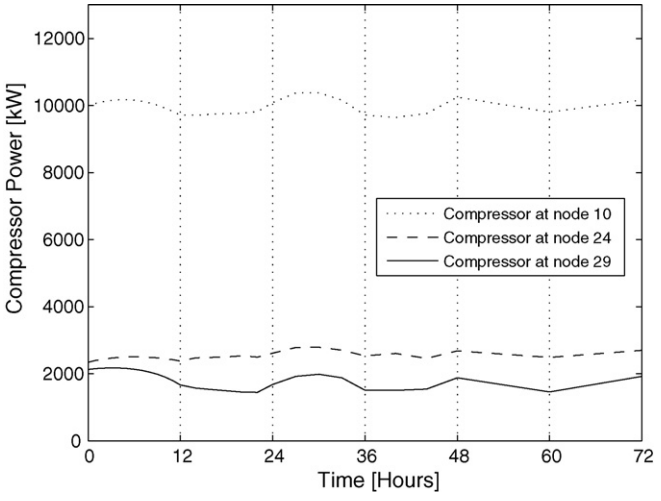

Fig. 14. Optimal compressor profiles for time of day electricity pricing and a regularization multiplier of 100.

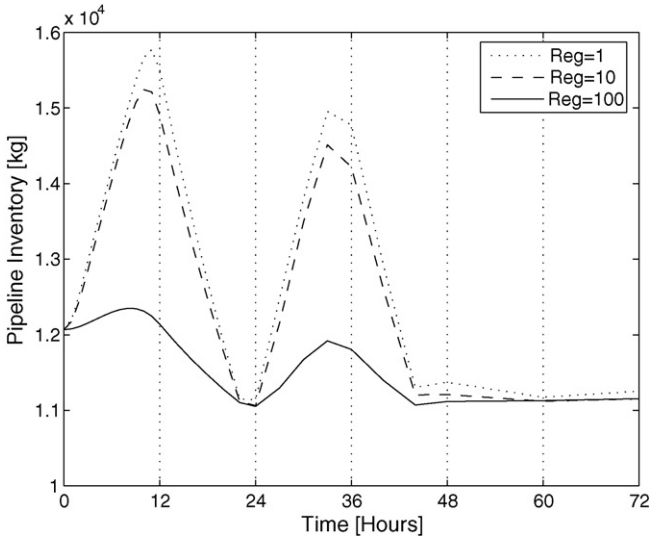

Fig. 15. Inventory profiles for time of day electricity pricing for the three different regularization multipliers considered.

the off-peak time periods. This is due to the fact that the demand charge is based on the larger of the maximum demand on-peak and half the maximum demand off-peak. For all three values of *Reg*, the NLP solver increases the compressor power and inventory during the initial off-peak time period. The compressor power and inventory then drop significantly during the next 12-h on-peak period. Use of the network inventory in this manner allows the compressor power to be reduced when electricity is expensive. This in principle can be utilized to reduce the overall energy costs associated with operation of industrial gas pipelines.

The economics of these optimal trajectories are compared to the flat rate base case scenarios in Table 4. Note that allowing more variation in the compressor profiles through the *Reg* parameter is essential to take advantage of time-of-day pricing. It can be seen from the table that for the smallest value of *Reg*, the time of day rate plan can save up to approximately $25,000 which corresponds to 5.13% on the electricity cost. The control profile appears to be implementable; however there are some small oscillations present. Increasing *Reg* to 10 results in only approximately $20,000 savings or 4.27%, but a much smoother control profile. Further, increasing *Reg* to 100 actually increases the utility cost by 0.02% over the flat rate case.

It should be noted that on the two examples with cost savings of 4.27% and 5.13%, the overall energy use increases by 0.42% and 0.41%. This is an interesting, but explainable result. The cost savings come from the reduction of the demand charge, so even though more electricity is being used, the total cost is less. Furthermore, more electricity is required to run the compressors in the time of day pricing runs because inventory is needed to get through the peak period and building inventory increases pipeline pressure, which in turn increases the compression power requirements.

5.2.4. Extensions to Real Time Pricing and Day Ahead Pricing

Finally, the model is extended to Real Time Pricing and Day Ahead Pricing. This is done by considering a uniform time discretization where the 48 h are represented by 1-h time periods. The pricing for each of the time periods are either known (provided by the utility company) or estimated using a forecasting model or a combination of these, such as in Ierapetritou et al. (2002). Unlike the previous cases, this pricing scheme does not include a demand charge. Additionally since there exists a significant cost to the inventory in the network, we can assume that inventory is not built-up in the network for more than about 24 h, before it is depleted to satisfy customer demands. These conditions allow the Real Time Pricing case study to consider only 48 h.

$$min \quad \frac{EC}{1000} + 0.1 \times \delta + 10^6 \sum_{d \in D, t \in T} q_{d,t}^{slack} \tag{30a}$$

$$s.t. \quad EC = \sum_{s \in S, t \in T \setminus \{t_f\}} \frac{1}{2}(Power_{s,t} + Power_{s,t+1})(t_{t+1} - t_t) cost_t \tag{30b}$$

$$\delta = \sum_{s \in S, t \in T \setminus \{t_f\}} \left(\frac{Power_{s,t+1} - Power_{s,t}}{t_{t+1} - t_t} \right)^2 \tag{30c}$$

$$\text{Eqs. (3)–(23), (24), (26) and (27)} \tag{30d}$$

Note that the values of the cost coefficients $cost_t$ are different in value from the prior case studies. In particular, $cost_t$ takes a different value for every hour. Day Ahead cost data from 8 p.m. on July 1st to 8 p.m. on July 3rd, 2008 are used for the 48 h in this case study. The Day Ahead electricity prices are given in Fig. 16. In a similar manner, Real Time Pricing can be considered if a model forecasts the hourly prices at least 24 or 48 h ahead. This methodology was tested with historical Day Ahead data, which is itself just a forecast of the spot price. The optimal compressor power trajectory is given in Fig. 17. The optimization required 233.29 s and 465 iterations with CONOPT. Just as in the prior case studies, the optimal solution involves an increase of compressor power when electricity is less expensive and a decrease of compressor power when electricity is expensive. Furthermore, the network inventory builds during the less expensive time periods and depletes during the more expensive time periods. The optimal network inventory profile is given in Fig. 18.

Quantifying cost savings with a Real Time Pricing scheme is problematic as the cost savings depends on the data set chosen for comparison. The data used in this study are historical data believed to be typical of a mid-summer's day for the Ameren utility company. The optimal energy cost for this 48-h period is $39,165.17.

Table 4
Summary of cost, break down of cost, energy usage, and demand for flat rate and time of day electricity pricing case studies.

	Reg = 100		Reg = 10		Reg = 1	
	Flat rate	ToD rate	Flat rate	ToD rate	Flat rate	ToD rate
Monthly cost	$454,306.29	$454,414.55	$454,237.92	$434,864.22	$454,207.67	$430,925.80
Customer charge	217.25	231.42	217.25	231.42	217.25	231.42
Demand charge	207,580.69	197,365.48	207,580.69	177,143.55	207,580.69	173,319.64
Energy charge	246,508.36	256,817.65	246,439.99	257,489.26	246,409.74	257,374.74
On-peak energy	5,135,701	5,130,817	5,134,819	5,115,555	5,136,239	5,106,751
Off-peak energy	5,135,481	5,143,752	5,133,514	5,195,531	5,130,833	5,201,947
Total energy	10,271,182	10,274,569	10,268,333	10,311,087	10,267,072	10,308,698
On-peak demand	14,466	13,754	14,466	12,344	14,466	12,078
Off-peak demand	14,466	15,830	14,466	17,555	14,466	17,822
Demand billed	14,466	13,754	14,466	12,344	14,466	12,078

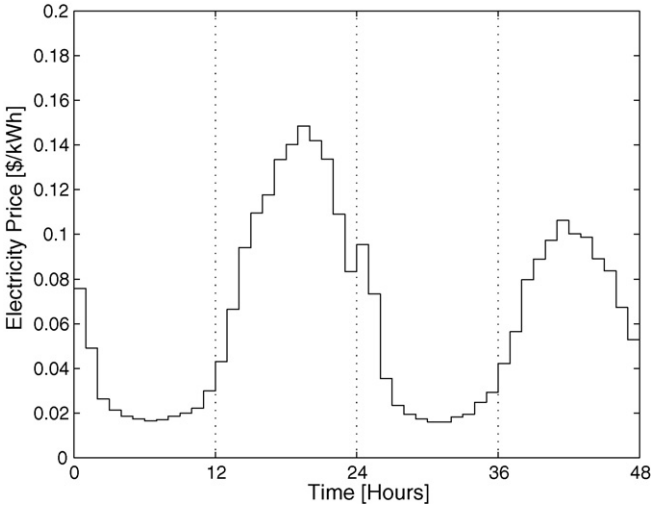

Fig. 16. Electricity prices used for Day Ahead Pricing case study.

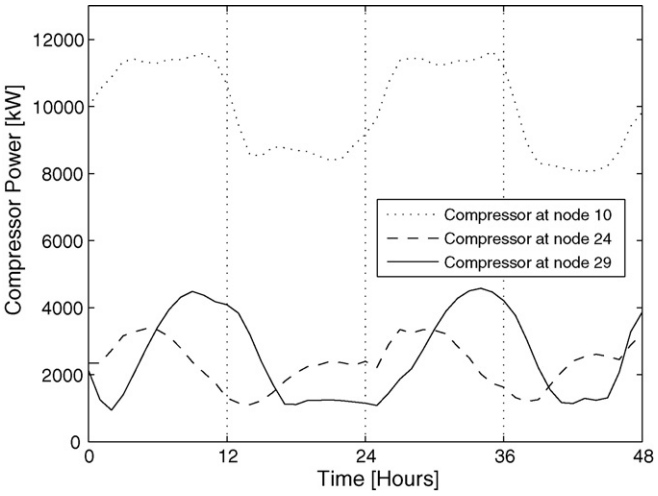

Fig. 17. Optimal compressor profiles for Day Ahead Pricing case study.

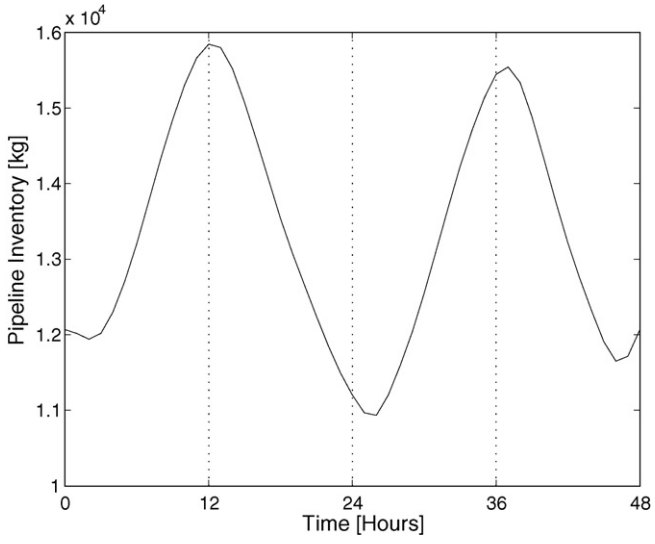

Fig. 18. Optimal network inventory for Day Ahead Pricing case study.

In contrast, had the NLP solver minimized total energy used without regard to the cost of the energy, the energy cost would have been $44,938.14. By taking into account the time dependence of the cost of energy, savings of 12.85% are realized, even though the total energy increases by 3.94%, from 684,769.549 kWh to 711,748.779 kWh.

6. Conclusions

MPEC and standard NLP optimization techniques have been applied to optimize problems with complex energy pricing scheme. Formulations are proposed for time of day, tiered pricing, maximum demand charge, and rank ordering. These formulations were applied to a oxygen pipeline network. The results show that by utilizing the pipeline inventory and time of pricing, the energy costs can be reduced by 4.27–5.13%, even though the overall energy usage increased by 0.41%. This is on a monthly utility bill of approximately $450,000, which results in $250,000 annual savings for the compression costs. Furthermore, cost savings of up to 12.85% are demonstrated by minimizing operating cost instead of energy consumption for Real Time Pricing, even though the total energy used increases by 3.94%. It is important to note that the pipeline network model does not take into account time dependencies or cost associated with the production of oxygen, only the compression costs. It is expected that cost savings could be increased further if production costs of oxygen would be included in the energy optimization, along with the ability to liquefy and store product.

Acknowledgments

Funding from the National Science Foundation (Grant CTS-0438279) and the Pennsylvania Infrastructure Technology Alliance (PITA) is gratefully acknowledged. Also, we are pleased to acknowledge the support of the Decision Sciences group at Air Products for hosting two summer internships for BTB. Finally, we offer our gratitude to Drs. Ken Anselmo and Mark Daichendt for insightful and interesting discussions and advice on this study.

References

Ameren, Electric Full Service Rates for AmerenUE, http://www2.ameren.com/business/Rates/ratesBundledElecFullSrvMO.aspx/

Ameren, Real Time Prices. http://www2.ameren.com/RetailEnergy/realtimeprices.aspx.

Anitescu, M., Tseng, P., & Wright, S. J. (2007). Elastic-mode algorithms for mathematical programs with equilibrium constraints: Global convergence and stationarity properties. *Mathematical Programming*, *110*, 337–371.

Batey, E. H., Courts, H. R., & Hannah, K. W. (1961). Dynamic approach to gas-pipeline analysis. *Oil & Gas Journal*, *59*, 65–78.

Baumrucker, B. T., Renfro, J. G., & Biegler, L. T. (2008). MPEC problem formulations and solution strategies with chemical engineering applications. *Computers and Chemical Engineering*, *32*, 2903–2913.

Drud, A. (2004). *CONOPT solver manual*. Washington, DC: GAMS Development Corporation.

Finlayson, B. A. (2003). *Nonlinear analysis in chemical engineering*. Seattle: Ravenna Park Publishing.

Fletcher, R., & Leyffer, S. (2004). Solving mathematical programs with complementarity constraints as nonlinear programs. *Optimization Methods and Software*, *19*(1), 15–40.

Hu, X. M., & Ralph, D. (2004). Convergence of a penalty method of mathematical programming with complementarity constraints. *Journal of Optimization Theory and Applications*, *123*(2), 365–390.

Ierapetritou, M. G., Wu, D., Vin, J., Sweeney, P., & Chigirinskiy, M. (2002). Cost minimization in an energy-intensive plant using mathematical programming approaches. *Industrial & Engineering Chemistry Research*, 41.

Kameswaran, S., Staus, G., & Biegler, L. T. (2005). Parameter estimation of core flood and reservoir models. *Computers and Chemical Engineering*, *29*(8), 1787–1800.

Larnaes, G. (2004). Models and scheduling tools help pipelines carry more nominated gas. *Pipeline and Gas Journal*, *231*(2), 33–34.

Leyffer, S., Lopez-Calva, G., & Nocedal, J. (2006). Interior methods for mathematical programs with complementarity constraints. *SIAM Journal of Optimization*, *17*(1), 52–77.

Marqués, D., & Morari, M. (1988). On-line optimization of gas pipeline networks. *Automatica*, *24*(4), 455–469.

Raghunathan, A., & Biegler, L. T. (2003). MPEC formulations and algorithms in process engineering. *Computers and Chemical Engineering*, *27*, 1381–1392.

Raghunathan, A., Diaz, M. S., & Biegler, L. T. (2004). An MPEC formulation for dynamic optimization of distillation operation. *Computers and Chemical Engineering*, *28*(10), 2037–2052.

Raghunathan, A. U., & Biegler, L. T. (2005). Interior point methods for mathematical programs with complementarity constraints (MPCCs). *SIAM Journal of Optimization*, *15*(3), 720–750.

Raghunathan, A. U., Perez-Correa, J. R., Agosin, E., & Biegler, L. T. (2006). Parameter estimation in metabolic flux balance models for batch fermentation—formulations and solution using differential variational inequalities. *Annals of Operations Research*, *148*, 251–270.

Ralph, D., & Wright, S. J. (2004). Some properties of regularization and penalization schemes for MPECs. *Optimization Methods and Software*, *19*(5), 527–556.

Shobrys, D. E., & White, D. C. (2000). Planning, scheduling and control systems: Why can't they work together? *Computers and Chemical Engineering*, *24*, 163–172.

van den Heever, S. A., & Grossmann, I. E. (2003). A strategy for the integration of production planning and reactive scheduling in the optimization of a hydrogen supply network. *Computers and Chemical Engineering*, *27*, 1813–1839.

Zhu, G.-Y., Henson, M. A., & Megan, L. (2001). Dynamic modeling and linear model predictive control of gas pipeline networks. *Journal of Process Control*, *11*, 129–148.